

ION PROBE ANALYSIS OF ARTIFICIALLY IMPLANTED IONS IN TERRESTRIAL SAMPLES AND SOLAR WIND IMPLANTED IONS IN LUNAR SURFACE SAMPLES, E. Zinner, The Lunar Science Institute, Houston, TX 77058 USA and McDonnell Center for the Space Sciences, Washington University, St. Louis, MO 63130 USA; R. M. Walker, McDonnell Center for the Space Sciences, Washington University, St. Louis, MO 63130 USA; J. Chaumont and J. C. Dran, Laboratoire René Bernas, University of Paris, 91406 Orsay, France.

We have previously reported ion-probe studies of depth profiles of implanted ions in terrestrial analogs (1). Here we report on extensions of these implantation experiments. We also give the first ion-probe measurements of naturally implanted solar wind ions in a lunar surface crystal. These permit comparison between solar wind, solar flares, and micrometeoroid fluxes in a given grain.

I. Analog experiments: a) Depth profiles (energy). Previous depth profiles had a long tail and did not correspond to calculated distributions. Three sources of this shape were investigated: diffusion by beam heating, knock-on effects in the implanting beam, and knock-ons by the ion-probe beam. Polished labradorite sections were implanted with  $^{13}\text{C}$  and  $^{52}\text{Cr}$  and ilmenites with  $^{23}\text{Na}$  and  $^{29}\text{Si}$  at 1.2 keV/nuc, total fluences from  $5 \times 10^{13}$  ions/cm<sup>2</sup> to  $5 \times 10^{15}$  ions/cm<sup>2</sup> and dose rates varying from  $1.25 \times 10^{12}$  ions/cm<sup>2</sup>/sec to  $1.5 \times 10^{13}$  ions/cm<sup>2</sup>/sec. No dependence of the depth profiles on the dose rate was seen, eliminating beam heating as a cause. Triply irradiated samples ( $^{52}\text{Cr}$ - $^{13}\text{C}$ - $^{53}\text{Cr}$  for labradorite and  $^{29}\text{Si}$ - $^{23}\text{Na}$ - $^{30}\text{Si}$  for ilmenite) were used to study the knock-on of the first implanted ion by a high dose of the second nuclide. At the dose used (e.g.,  $3 \times 10^{16}$   $^{13}\text{C}$ /cm<sup>2</sup>) the effect is small but still noticeable. Broadening produced by self knock-ons was observed at large doses ( $10^{17}$   $^{12}\text{C}$ /cm<sup>2</sup> in labradorite and  $5 \times 10^{16}$   $^{29}\text{Si}$ /cm<sup>2</sup> in ilmenite) of a single implanted nuclide. The results show that self-broadening of an implanted solar wind species is negligible for all elements of interest. The strongest effect was produced by the analyzing beam itself (2). The use of  $^{16}\text{O}$  at 15 kV (0.94 keV/nuc) results in a long tail (Fig. 1; the 0 dose at the maximum of the depth profile is  $\sim 1.2 \times 10^{18}$   $^{16}\text{O}$ /cm<sup>2</sup>) whereas profiles with an  $\text{NO}_2$ -beam at 9 kV (0.2 keV/nuc) closely approximate the theoretically expected shape. We conclude that it is possible to use depth profiles to measure the energy of solar wind implanted ions.

b) Retention. No losses were observed in labradorite implanted with up to  $10^{17}$   $^{12}\text{C}$ /cm<sup>2</sup> and ilmenite with up to  $5 \times 10^{16}$   $^{29}\text{Si}$ /cm<sup>2</sup>. A more realistic simulation of the lunar radiation environment, the combined implantation of  $10^{18}$  H/cm<sup>2</sup>,  $10^{18}$  He/cm<sup>2</sup> (corresponding to a lunar exposure time of 15,000 yrs) together with  $^{13}\text{C}$  and  $^{52}\text{Cr}$  was studied in labradorite, together with  $^{23}\text{Na}$  and  $^{29}\text{Si}$  in Mn-rich haematite (oxidized sections of ilmenite). Depth profiles from the first case (Fig. 2) show a very small effect of the H and He irradiation. The Na and Si distributions in haematite were much more affected by the additional H and He irradiations, but this needs to be confirmed in ilmenite. We conclude that quantitative retention of solar wind implanted ions may be expected in lunar feldspars.

c) Annealing effects. A labradorite sample implanted with  $^{52}\text{Cr}$  was annealed at increasing temperatures (3 hrs each in Ar-atmosphere). The

## ION PROBE ANALYSIS OF SOLAR WIND

Zinner, E. et al.

depth profiles after each heating step are seen in Fig. 3. Only a modest diffusion occurs at 770°C, indicating that modification of implantation profiles should be negligible at ambient lunar temperatures. When diffusion does occur, however, it is not a simple process: the implanted species migrates preferentially to the surface and apparently more than one activation energy is involved.

II. Analysis of 76215,77. 76215,77, a 0.3 mm long plagioclase crystal from the surface of 76215,32, has a microcrater density ( $>.1\mu$ ) of  $5 \times 10^6/\text{cm}^2$  (1,3) showing that it was exposed to free space. Previous estimates of exposure age based on solar flare tracks gave  $\sim 1.6 \times 10^4$  yrs (3,4). After preliminary depth profiles showed surface enhancements at the masses 54 ( $^{54}\text{Fe}$ ), 52 ( $^{52}\text{Cr}$ ), 48 ( $^{48}\text{Ti}$ ), 31 ( $^{31}\text{P}$ ), 24 ( $^{24}\text{Mg}$ ), and 12 ( $^{12}\text{C}$ ), the crystal was implanted with  $^{57}\text{Fe}$ ,  $^{53}\text{Cr}$ ,  $^{25}\text{Mg}$ , and  $^{13}\text{C}$  at 1 keV/nuc for internal calibration of the enhanced species. Profiles of one of the runs after these implantations are shown in Fig. 4. The similarity of the profiles of natural enhancements and artificially implanted ions gives strong evidence that the surface enhancements are due to solar wind implanted ions. In order to investigate the problem of molecular interferences, high resolution (2500) mass scans were taken as a function of time for the masses in question with a CAMECA IMS 300. Only a single mass peak was seen at 24, 25 and 48, 49 (in all cases this peak decreased with sputtering time). Masses 52 and 53 showed a more complex peak structure (in addition to  $^{52}\text{Cr}$  and  $^{53}\text{Cr}$  tentatively identified as  $^{40}\text{CaC}$ ,  $\text{C}_4\text{H}_4$  and  $^{40}\text{CaCH}$ ,  $\text{Na}^{30}\text{Si}$ ,  $\text{C}_4\text{H}_5$  respectively), however, the pure element peaks dominated by a factor of 10. The largest molecular peaks were found at 56 ( $^{40}\text{CaO}$ ) and 54 ( $\text{Al}_2$ ), but only the low mass peaks ( $^{56}\text{Fe}$  and  $^{54}\text{Fe}$ ) were decreasing with time identifying the surface components as the atomic species. Table 1 shows the ratios of the peak heights of natural and implanted ions for all the ARL-runs made after the implantation in different areas on the crystal. The remarkable constancy of these ratios support the view that we are dealing with a general surface enhancement and not with local effects (pancakes or other glass splashes). Solar wind exposure ages derived from those ratios (with the present-day H-flux and Cameron's (5) elemental abundances) are shown in Table 2 where we added also P and Ti for which direct calibrations were not performed. These numbers are too high since it was assumed that naturally and artificially implanted ions were detected with the same sensitivity. In fact, 76215,77 was coated with  $\sim 100\text{\AA}$  of Au and a large fraction of the artificially implanted ions did not penetrate the Au-coating and thus were counted with less sensitivity than ions from the silicate (chemistry effect). There is a considerable spread between different elements (especially  $^{52}\text{Cr}$ ). On the other hand, these solar wind exposure ages (neglecting the unknown efficiency factor) are of the same order of magnitude as the track age. They thus constitute independent measurement of the micrometeoroid flux (3).

References. (1) Zinner, E., and Walker, R. M., 1975, Proc. Lunar Sci. Conf. 6th, p. 3601. (2) McHugh, J. A., 1974, Rad. Effects 21, p. 209. (3) Morrison, D. A., and Zinner, E., 1975, Proc. Lunar Sci. Conf. 6th, p. 3373. (4) Blanford, G. E., et al., 1975, Proc. Lunar Sci. Conf. 6th, p.3557. (5) Cameron, A. G. W., 1973, Space Sci. Rev. 15, p. 121.

ION PROBE ANALYSIS OF SOLAR WIND

Zinner, E. et al.

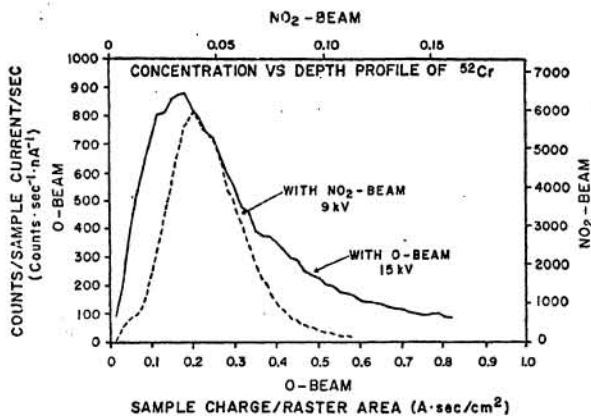


Fig. 1. Profiles in labradorite implanted with  $5 \times 10^{14}$   $^{52}\text{Cr}$  at 1.2 keV/nuc with O and  $\text{NO}_2$  ion probe beam.

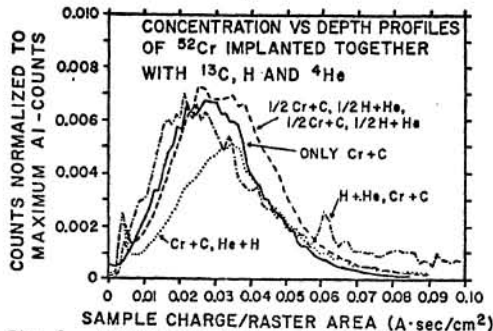


Fig. 2. Labradorite implanted with  $10^{18}\text{H}/\text{cm}^2$ ,  $10^{19}\text{He}/\text{cm}^2$ ,  $3 \times 10^{15} \text{ }^{13}\text{C}/\text{cm}^2$  and  $5 \times 10^{14} \text{ }^{52}\text{Cr}/\text{cm}^2$  in different sequences.

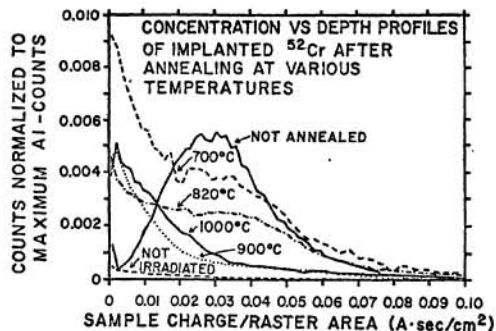


Fig. 3. Depth profiles of annealed labradorite implanted with  $5 \times 10^{14}$  ions/ $\text{cm}^2$  of  $^{52}\text{Cr}$  at 1.2 keV/nuc.

Table 1: Ratios of peak heights in 76215,77 depth profiles.

Run	54/57	52/53	24/25	12/13
Aug. 12.1	-	-	-	2.4
Aug. 13.1	0.26	4.1	3.5	2.8
Aug. 13.2	0.36	4.8	4.2	4.3
Nov. 2.1	-	5.0	-	1.9
Nov. 3.3	0.09	4.1	8.3	2.9
Nov. 4.1	-	4.0	3.2	2.5

Table 2: Solar wind exposure times from surface enhancements in 76215,77.

$^{54}\text{Fe}$	$5 \times 10^4$ years
$^{52}\text{Cr}$	$5 \times 10^5$ "
$^{24}\text{Mg}$	$1.3 \times 10^5$ "
$^{12}\text{C}$	$2.3 \times 10^4$ "
$^{48}\text{Ti}$	$1.5 \times 10^5$ "
$^{31}\text{P}$	$8 \times 10^4$ "

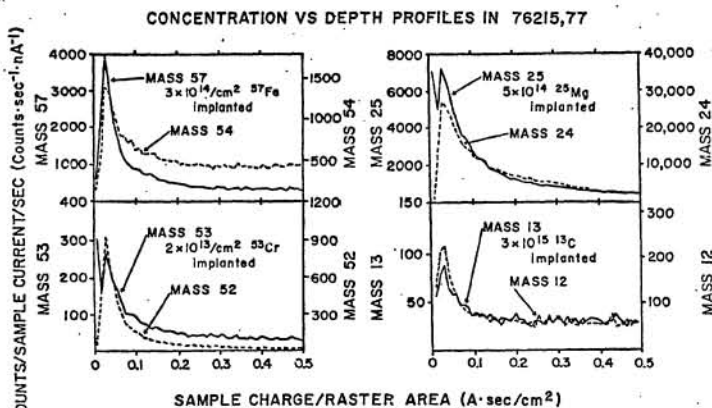


Fig. 4. Depth profiles of natural species together with implanted ions in 76215,77.